

Multiphasic effects of cholesterol on influenza fusion kinetics reflect multiple mechanistic roles

Marta K. Domanska,* Dominik Wrona,* and Peter M. Kasson*

*Departments of Molecular Physiology and Biological Physics and Biomedical Engineering, University of Virginia, Charlottesville, Virginia 22908, USA.

*Correspondence: kasson@virginia.edu

Supporting Information

Supplementary Materials and Methods

Pages 2-3

Supplementary Note

Page 4

Supplementary Figures

Pages 5-8

Supplementary Table

Page 9

Supplementary Materials and Methods

Materials.

Lipids: 1-Palmitoyl-2-oleoyl-*sn*-glycero-3-phosphocholine (POPC), 1-Palmitoyl-2-oleoyl-*sn*-glycero-3-phosphoethanolamine (POPE), 1,2-dioleoyl-*sn*-glycero-3-phospho-ethanolamine-N-(7-nitro-2-1,3-benzoxadiazol-4-yl) (NBD-DOPE), and 1,2-dioleoyl-*sn*-glycero-3-phosphoethanolamine-N-(lissamine rhodamine B sulfonyl) (ammonium salt) (Rh-DOPE) were purchased from Avanti Polar Lipids, Alabaster, AL and used without further purification.

Cholesterol, sodium chloride, sodium phosphate dibasic, sodium phosphate monobasic, citric acid, sodium hydroxide, methyl- β -cyclodextrin and other chemicals were purchased from Sigma, St. Louis, MO. Chloroform, ethanol, cell culture supplies (Fisher Scientific, Fair Lawn, NJ). Amplex Red Cholesterol Assay kit, ANTS and DPX were purchased from Life Technologies, Grand Island, NY. Purified X:31 influenza virus (A/Aichi/68 (H3N2)) was purchased from Charles River Laboratories.

Liposome preparation.

Large unilamellar vesicles (LUVs) at the specified compositions were prepared by extrusion and size exclusion chromatography as detailed below. Briefly, stock lipid solutions in chloroform were mixed in a glass test tube, dried under the argon stream and placed under vacuum for additional 1 to 2 hours. Next, the dried lipid film was hydrated with fusion buffer (FB buffer: 10 mM phosphate/90 mM citrate/150 mM NaCl, pH7.4) containing ANTS/DPX (12.5 mM ANTS/45 mM DPX) at a final lipid concentration of 2 mM. The mixture was vortexed for 5 to 10 min to form a multilamellar vesicle suspension, which was frozen and thawed five times in liquid nitrogen and a warm water bath. The multilamellar vesicle suspension was then extruded 15-20 times through two polycarbonate membranes of 100 nm pore size. In the final step, the LUVs were purified on a G50 superfine column to remove the unencapsulated ANTS and DPX. To ensure vesicle stability, osmolarity of all buffers was measured and adjusted using a cryoscopic osmometer (Osmomat 030, Gonotec).

Cholesterol determination.

The cholesterol content of influenza virus membranes was estimated using an Amplex Red Cholesterol Assay Kit according to the manufacturer's instructions. Virus was measured at 2 mg/ml. Briefly, 50 μ L of 0, 10 mM, 20 mM and 50 mM M β CD treated virus and untreated virus, each containing 22 μ g viral protein per sample were resuspended in Amplex Red working buffer. After a 30-60 min incubation, fluorescence was measured using excitation, emission and cutoff wavelengths of 560, 590, and 570 nm, respectively. Samples with saturating signal were re-run at 2x or 10x lower viral protein content and corrected accordingly.

Cholesterol replenishment of M β CD-treated influenza virus.

Cholesterol-depleted influenza virus was treated with previously prepared water-soluble cholesterol:M β CD complex. The complex was prepared by dissolving M β CD in 50mM Tris pH 7.5, addition of solid cholesterol and overnight vortexing. The solution was filtered to remove insoluble cholesterol crystals, and the ratio of cholesterol to M β CD was estimated (values ranged between 1.5:40 and 2:40). The virus was mixed with this complex at a 1:1 ratio, and Tris buffer

was added to obtain a final concentration of 10mM M β CD. The mixture was incubated at 37°C for 30 minutes, centrifuged at 4° C and 14000 rpm for 40 minutes, and resuspended in the fusion buffer. The kinetics of fusion between such treated virus and liposomes containing 20 mol% cholesterol were measured as described previously. The concentration of cholesterol was estimated using the Amplex Red assay.

Viral lipid extraction.

Viral lipid was extracted from the viral particles via the Bligh and Dyer extraction procedure (1). Briefly, 80 μ l of virus at 2mg/ml was mixed with methanol-HCl/chloroform mixture at a 1:2:0.8 v/v/v ratio. After one hour incubation at room temperature, 100 μ L of water and chloroform each were added to the mixture and spun down for 30 seconds at 14000 rpm. The organic layer was removed and transferred to a glass tube. The upper aqueous layer was re-extracted with 200 μ L of chloroform and again spun down for 30 seconds at 14000 rpm. Again, the bottom layer was removed and combined with previous organic layer. Finally, the organic fraction was re-purified by back-extraction with 760 μ L of chloroform/methanol-HCl/water mixture. The aqueous layer was removed by aspiration after a brief spin. The remaining organic layer containing viral lipids was dried in a speed-vac. Dried viral lipids were then used directly for phosphate analysis.

Phosphate assay.

Analysis of phospholipids were performed using a standard phosphate assay, where lipids were digested with perchloric acid and the released phosphate was reacted with ammonium molybdate in the presence of reducing agent, such as ascorbic acid, forming a blue complex. The amount of the phosphate complex was measured by absorbance at 820 nm and compared to the standard inorganic phosphate. For viral phospholipid assessment, previously extracted lipids were mixed with 10 μ L of 2% ammonium molybdate, vortexed and dried in a speed-vac for 30 min. Then 300 μ L of 70% perchloric acid was added to the glass tube, and the tube was heated at 180 °C for 30 min. After tube was cooled to room temp, 1.5 mL of 0.4 % ammonium molybdate and 0.22 mL of 10% (w/v) ascorbic acid were added, vortexed and heated for 10 min at 90° C. Tubes were cooled down to room temp for 20 min and absorbance at 820 nm was measured. Standard were assayed using inorganic phosphate: 0, 10, 50, 100 and 125 μ L of 1mM K₂HPO₄ solution.

Hemagglutination titers.

A standard hemagglutination assay (2) was performed. Serial twofold dilutions of the virus sample were made in the PBS buffer and placed on a V-bottom plate. Next 0.5% (v/v) chicken red blood cells were added to each well at 1:1 (v:v) virus to blood cell ratio. The plate was incubated for 1 hour at 4°C. The HA titer was defined as the most diluted viral sample that formed a lattice rather than a distinct blood cell spot at the bottom of the well.

Supplementary Note

Control experiments to calculate the fraction of contents signal attributable to contents leakage were performed as follows. 100 nm liposomes were prepared with molar ratios 30:47:20:1.5:1.5 POPE:POPC:Cholesterol:NBD-DOPE:Rh-DOPE encapsulating ANTS only rather than ANTS/DPX complex. Fusion experiments with X-31 influenza virus were run on four pairs of samples with 0 and 36 mM DPX respectively in the external buffer. Fluorescence intensity values I_0 , I_{plateau} , and I_{max} were recorded at the time of acidification, plateau value during the fusion reaction (taken as the average value over minutes 12-15), and lysis with 1% Triton X-100. The fluorescence signal due to ANTS leakage was estimated as the difference: $(I_{\text{plateau-DPX}} - I_{0\text{-DPX}}) - (I_{\text{plateau+DPX}} - I_{0\text{+DPX}}) = I_{\Delta}$. This is the fluorescence intensity increase upon fusion that is present without DPX quencher in the buffer but missing when DPX quencher is present. In the case of leakage, DPX could also leak into the liposomes, which would decrease signal. The above difference I_{Δ} is thus an upper bound on the leakage intensity when considering DPX leakage. Intensity values I_{Δ} were converted to ANTS concentration in the external compartment using an ANTS standard curve measured under the same buffer conditions. A second standard curve with ANTS and 30 mM DPX in the external compartment showed 89 ± 1 % quenching by DPX at the calculated ANTS concentration. Taking into account this quenching, the concentration of leaked ANTS in the external compartment was estimated at 420 ± 3 nM.

A standard phosphate assay yielded a phospholipid concentration of approximately 1.2 mM. Using the approximate diameter of the vesicles (110 ± 10 nm as determined by dynamic light scattering), a spherical geometry approximation, and an estimate of the area per phospholipid head group and cholesterol (tested over the range over the range $50\text{-}60 \text{ \AA}^2$ per phospholipid and $12\text{-}14 \text{ \AA}^2$ per cholesterol), we can estimate the vesicle contents volume at $0.10 \mu\text{L}$ in the $150 \mu\text{L}$ fusion reaction. We can then derive the approximate concentration of encapsulated ANTS to be $6.8 \mu\text{M}$ when averaged over the full reaction volume. This would correspond to 6.2% vesicle contents leakage (5.7% to 6.8% depending on the lipid area estimate). Using a series of experiments under the same conditions as above except with encapsulated ANTS/DPX and DPX in the external compartment, this level of leakage is calculated to result in a fluorescence signal of 1.18 intensity units, or 8.7 ± 0.1 % of the observed $(I_{\text{plateau}} - I_0)$ value. The remaining 91.3% of signal upon fusion is thus estimated as due to contents mixing. This estimate relies on a large number of approximations, but it suggests that the ANTS/DPX encapsulation scheme we use with DPX quencher in the buffer is largely successful at suppressing leakage signal.

Supplementary Figures

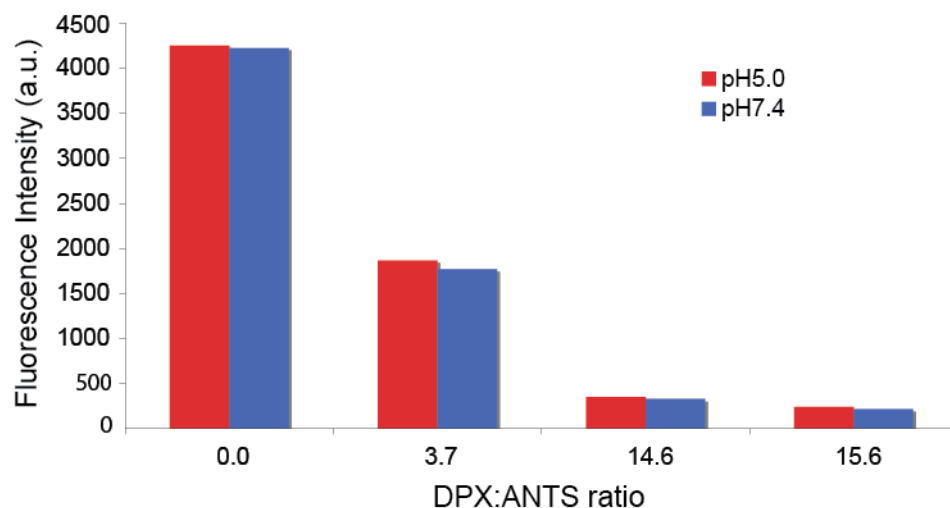


Figure S1. Solution quenching of ANTS fluorescence by DPX. ANTS fluorescence emission at 530 nm was measured for solutions containing 2.3 mM ANTS and 0, 8.6, 34, or 36 mM DPX. 2.3 mM ANTS is a loose upper bound on the final ANTS concentration were all encapsulated ANTS to leak into the reaction buffer during a fusion experiment. If full leakage occurred the final DPX concentration would be ~34 mM (14.6 DPX:ANTS ratio), resulting in >90% quenching of ANTS fluorescence. A more precise calculation (although one involving several approximations) is given in the Supplemental Note above and suggests that the actual concentration after full leakage would be closer to 7 μ M.

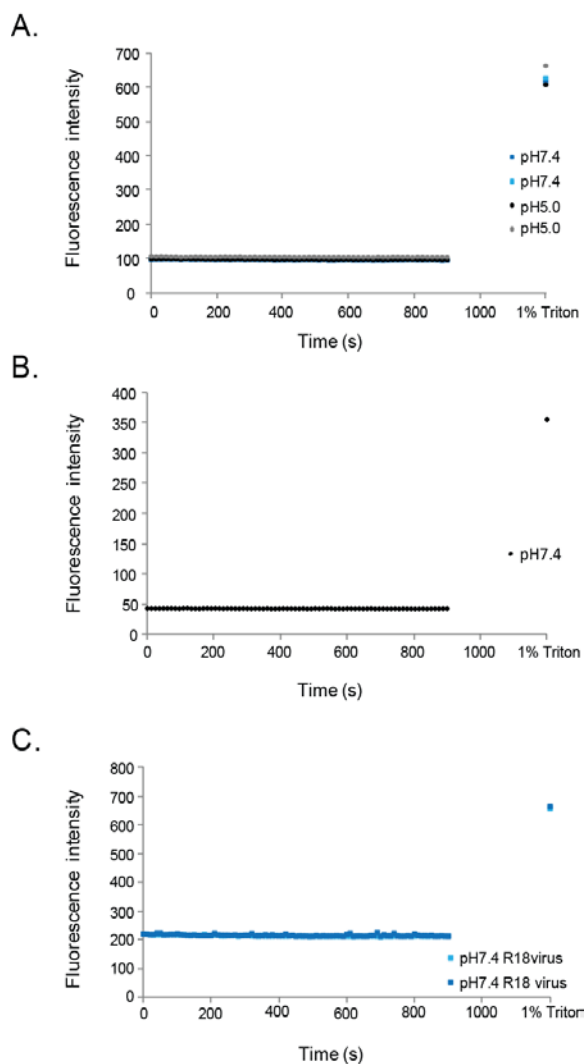


Figure S2. Labeled lipids do not detectably transfer in the absence of fusion.

Plotted are a series of control experiments to test for labeled lipid transfer between pairs of 100 nm vesicles or between vesicles and X:31 influenza virus under nonfusogenic conditions. Panel **A** shows duplicate fluorescence traces for a mixture of labeled and unlabeled vesicles incubated at either pH 5.0 or pH 7.4. Vesicles containing 20 mol % cholesterol were labeled with 1.5 mol % each of NBD-DOPE and Rh-DOPE. Panel **B** shows a similar trace for labeled vesicles and unlabeled virus under the conditions used for fusion except that the pH was maintained at 7.4. Panel **C** shows a similar experiment except that unlabeled vesicles were incubated with X:31 virus that had been labeled with R18 dye. All lipid dyes were loaded at quenching concentrations; a final time point in each panel shows the fluorescence increase upon addition of 1% Triton X-100. Under none of these conditions did we observe non-fusion transfer of dye (which would manifest as an increase in fluorescence) on the time scale of our fusion experiments. R18 dye would be expected to undergo some such transfer on substantially longer timescales, however.

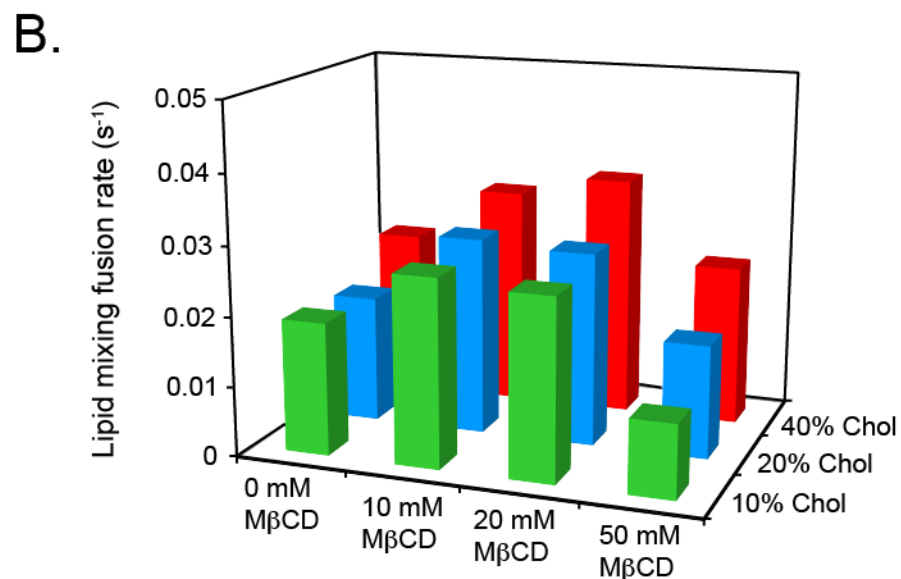
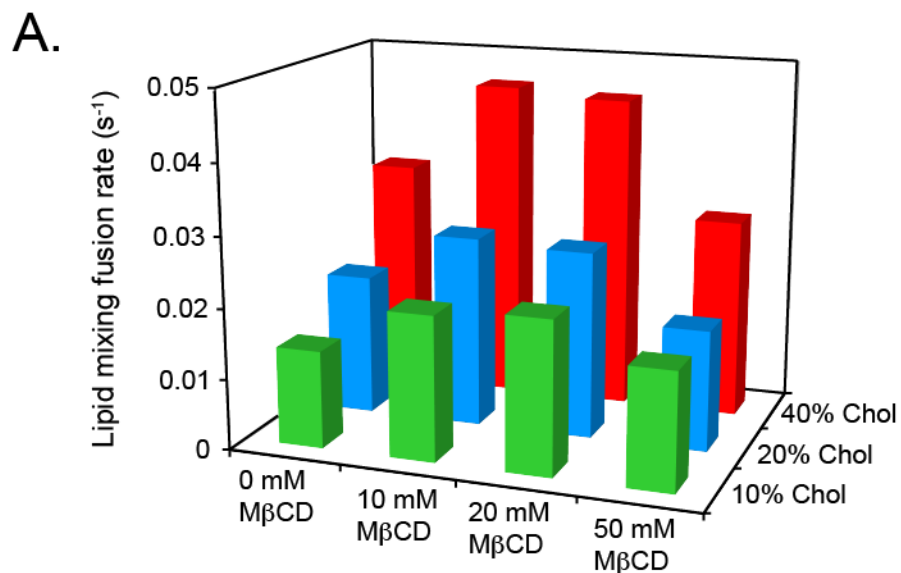


Figure S3. Fusion rates vary with cholesterol regardless of whether PC:PE ratio or PE mol % is held constant. Fusion experiments were performed either holding the mol % POPE fixed at 30% in target vesicles (panel **A**) or holding the POPC:POPE ratio fixed at 2:1 (panel **B**). The response of fusion rates to mol % cholesterol in target vesicles and to extraction of cholesterol from the virus is similar in both cases. Bars plotted represent the median of at least 3 experiments at each condition.

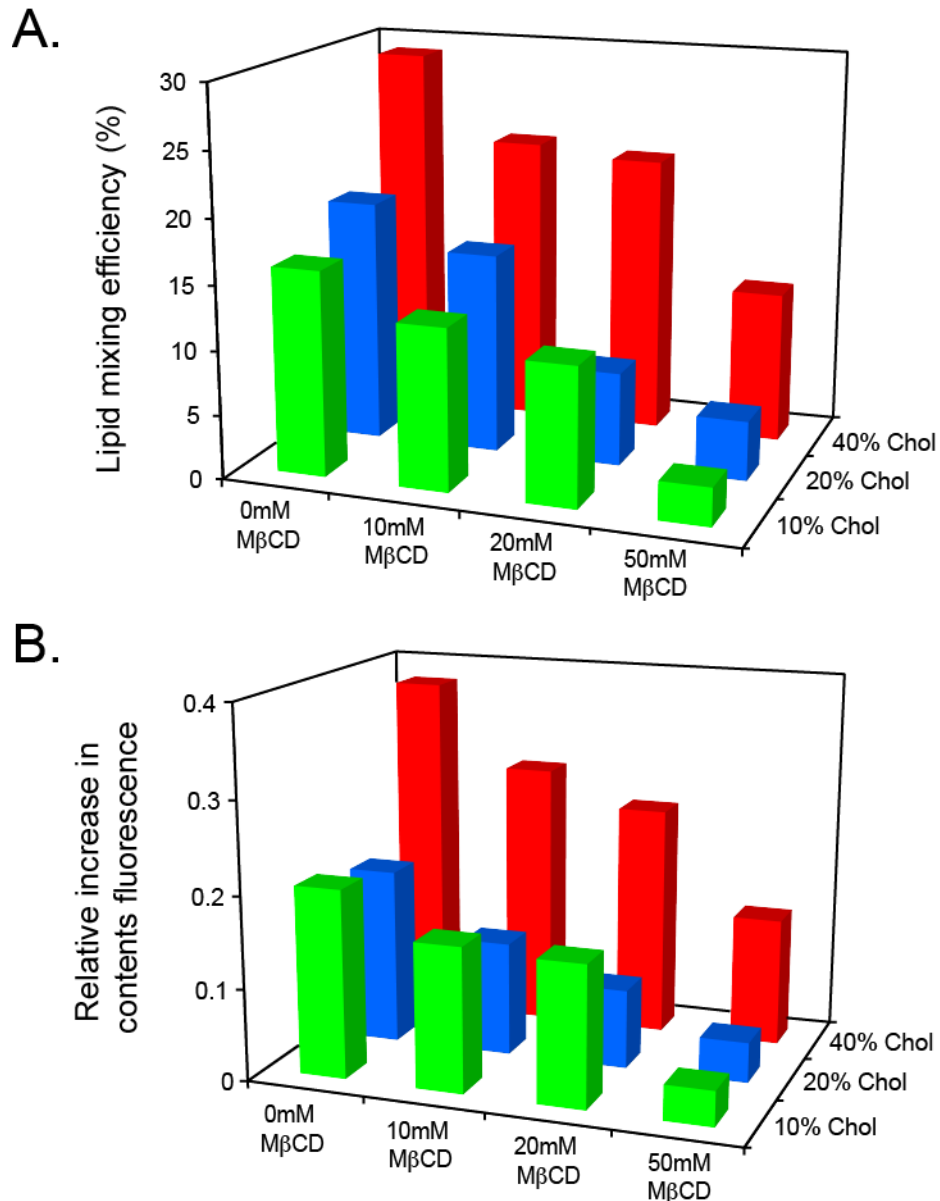


Figure S4. Extent of lipid and contents mixing shows a consistent decrease with decreasing cholesterol. Panel **A** shows lipid mixing efficiency values at each target vesicle composition and M β CD treatment tested. Panel **B** shows the extent of contents dye dequenching for the same conditions. Unlike fusion rates, efficiencies show a monotonic response to cholesterol to within error in either virus or target membrane, with lower cholesterol compositions reducing efficiency. Efficiency values were calculated from exponential fits to fluorescence dequenching traces as described in the Supporting Methods. Each bar represents the median of 5-13 independent experiments. Measurements at 10 mol % cholesterol had a larger error range, particularly for contents mixing.

Supplementary Table

Sample	ANTS fluorescence (a.u)	NBD fluorescence (a.u)
Prior to acidification	42	43
Fusion end product (15 min)	66	164
Purified vesicle fraction (normalized)	62	186
Volume-matched control, unpurified fusion end product	70	186

Table S1. Contents fluorescence in isolated vesicles after fusion..

A fusion reaction between X:31 influenza virus and 100 nm vesicles containing 20 mol % cholesterol was performed. After 15 minutes, a sample was added to a 1.2 mL Sephadex G50 spin column and spun at 4° C and 1000 x g for 2 minutes. The purified vesicle fraction eluted from the column was volume-matched to a control set of fusion end products that was maintained at 4° C after the 15-minute fusion reaction at 37° C rather than undergoing purification. Samples were also normalized for column yield using NBD fluorescence. The purified sample of fusion products (and unfused reactants) accounts for 86% of the fluorescence increase observed during the fusion reaction. Since this experiment did not control for vesicle leakage during purification, only lipid loss, the intra-luminal fluorescence at the end of the fusion reaction is likely even higher than this.

Supporting References.

1. Bligh, E. G., and W. J. Dyer. 1959. A rapid method of total lipid extraction and purification. *Can J Biochem Physiol* 37:911-917.
2. Hirst, G. K. 1942. The Quantitative Determination of Influenza Virus and Antibodies by Means of Red Cell Agglutination. *J Exp Med* 75:49-64.